International Journal of Modern Physics E
Vol. 25 (2016) 1650062 (21 pages)

DOI: 10.1142/S0218301316500622

Nuclear structure and decay properties of even–even nuclei in $Z = 70-80$ drip-line region

S. Mahapatro*,‡, C. Lahiri†,§, Bharat Kumar†,
R. N. Mishra* and S. K. Patra†

*Department of Physics, Ravenshaw University, Cuttack 753003, India

†Institute of Physics, Sachivalaya Marg, Bhubaneswar-751005, India
‡narayan@iopb.res.in
§clahiri@iopb.res.in

Received 2 March 2016
Revised 20 June 2016
Accepted 30 June 2016
Published 2 August 2016

We study nuclear structure properties for various isotopes of Ytterbium (Yb), Hafnium(Hf), Tungsten(W), Osmium(Os), Platinum(Pt) and Mercury(Hg) in $Z = 70$–80 drip-line region starting from $N = 80$ to $N = 170$ within the formalism of relativistic mean field (RMF) theory. The pairing correlation is taken care by using BCS approach. We compared our results with finite range droplet model(FRDM) and experimental data and found that the calculated results are in good agreement. Neutron shell closure is obtained at $N = 82$ and 126 in this region. We have also studied probable decay mechanisms of these elements.

Keywords: Relativistic mean field; deformed nuclei; neutron separation energy; potential energy surface; single particle levels; decay modes.

PACS Number(s): 21.10.Dr, 21.10.Pc, 21.10.Tg, 23.40.−s, 23.60.+e

1. Introduction

Recent developments of radioactive ion beam (RIB) facilities have encouraged various experimental as well as theoretical developments for nuclei far from the β stability line. Physics of nuclear structure and decay mechanism in neutron rich nuclei is a very popular field of study in present days.[1,2] Recently, the study of deformed nuclear shapes is also a very interesting topic and a number of excellent review articles exist[3–6] in this context. In literature, after the early calculations, which have predicted the existence of the superdeformed shape (see Ref. 2 for the review),

§Corresponding author.

its first experimental discovery took place in 1985.[7] Till then, numerous groups developed sophisticated techniques to perform calculations allowing the description of rotational bands for very elongated shapes. The phenomenon of superdeformation constitutes a spectacular manifestation of the mean-field properties of nuclei.

The change of shape of nuclei and other properties of nuclear structure with neutron number has attracted much theoretical and experimental attention for many years.[8–12] The conditions needed for the observation of shapes coexisting in such nuclei have been a matter of challenge and theoretically calculated by Patra and Panda[13] in 1993. The change of shapes of Pt isotopes was studied by Sharma and Ring.[14] The shapes of nuclei such as Os and Pt has also been studied by using the Hartree–Fock–Bogoliubov (HFB) formalism within the nonrelativistic framework.[8] Recently, Kumar *et al.*[15] studied the shape co-existence in Zr isotopes.

The nuclei with $Z = 70-80$ consist of both Rare Earth Metals (Yb) as well as the Transition metals(Hf, W, Os, Pt, Hg). They manifest a lot of interesting phenomena like shape co-existence, change of shape in an isotopic chain etc.[16,17] In this region of the atomic number, variety of shapes such as prolate, oblate and spherical configuration of nuclei appear in ground state.[18]

Many theoretical as well as experimental papers have focused their interest on the shape transition,[19] shape isomerism and the observation of superdeformed bands[20] in neutron-deficient Hg isotopes.

The aim of this paper is to explore the neutron rich side of the concerned mass region with RMF formalism. Mainly, the structure information like deformation, two-neutron separation energy, single particle energy levels etc. has been extracted using NL3 force parameter.

Further, α decay has been remained a very powerful tool to study the nuclear structure since its discovery by Becquerel in 1896. We also find other exotic decay modes like β decay, spontaneous fission, cluster-decay, etc. Therefore, it will be interesting to see the preferred decay modes of these neutron-rich even–even nuclei.

The paper is organized as follows. In Sec. 2, we have given a brief outline about the relativistic mean field (RMF) formalism. The effects of pairing for open shell nuclei, included in our calculations, are also discussed in this section. Our results are discussed in Sec. 3. The reaction Q values for α and β decay and their corresponding half-lives are given in Sec. 4. A concluding remark is given in Sec. 5.

2. Theoretical Framework for Relativistic Mean Field Model

The RMF model[21–28] is a well applied technique in recent years and has been applied to finite nuclei and infinite nuclear matter. In the present work, we have taken the RMF Lagrangian[21] with NL3 parameter set[29] in our study. This force parameter set is successful in both β-stable and drip-line nuclei. The Lagrangian contained the term of interaction between meson and nucleon and also self-interaction of isoscalar–scalar *sigma* meson. The other mesons are isoscalar-vector *omega* and isovector-vector rho mesons. The photon field A_μ is included to take care

of Coulombic interaction of protons. The pairing correlation is taken care by using Bardeen–Cooper–Schrieffer (BCS) approach.[21] We start with the relativistic Lagrangian density for a nucleon–meson many-body system,

$$\begin{aligned}\mathcal{L} = {} & \overline{\psi_i}\{i\gamma^\mu\partial_\mu - M\}\psi_i + \frac{1}{2}\partial^\mu\sigma\partial_\mu\sigma - \frac{1}{2}m_\sigma^2\sigma^2 \\ & - \frac{1}{3}g_2\sigma^3 - \frac{1}{4}g_3\sigma^4 - g_s\overline{\psi_i}\psi_i\sigma - \frac{1}{4}\Omega^{\mu\nu}\Omega_{\mu\nu} \\ & + \frac{1}{2}m_w^2V^\mu V_\mu + \frac{1}{4}c_3(V_\mu V^\mu)^2 - g_w\overline{\psi}_i\gamma^\mu\psi_iV_\mu \\ & - \frac{1}{4}\mathbf{B}^{\mu\nu}.\mathbf{B}_{\mu\nu} + \frac{1}{2}m_\rho^2\mathbf{R}^\mu.\mathbf{R}_\mu - g_\rho\overline{\psi}_i\gamma^\mu\boldsymbol{\tau}\psi_i.\mathbf{R}^\mu \\ & - \frac{1}{4}F^{\mu\nu}F_{\mu\nu} - e\overline{\psi}_i\gamma^\mu\frac{(1-\tau_{3i})}{2}\psi_iA_\mu. \end{aligned} \tag{1}$$

Here, sigma meson field is denoted by σ, omega meson field by V_μ and rho meson field is denoted by ρ_μ. In the equations, A^μ denotes the electromagnetic field, which couples to the protons. ψ are the Dirac spinors for the nucleons, whose third components of isospin is τ_3 and g_s, g_2, g_3, g_ω,c_3, g_ρ are the coupling constants. A definite set of coupled equations is obtained from the above Lagrangian and solved self-consistently in an axially deformed harmonic oscillator basis. The total energy of the system is given by the expression,

$$E_{\text{total}} = E_{\text{part}} + E_\sigma + E_\omega + E_\rho + E_c + E_{\text{pair}} + E_{\text{c.m.}}, \tag{2}$$

where E_{part} is the sum of the single-particle energies of the nucleons and E_σ, E_ω, E_ρ, E_c, E_{pair} are the contributions of the meson field, the coulomb field and the pairing energy, respectively. The center-of-mass (c.m.) motion energy correction is estimated by the harmonic oscillator formula $E_{\text{c.m.}} = \frac{3}{4}(41A^{-1/3})$ MeV, where A is the mass number of the nucleus. The total quadrupole deformation parameter β_2 and hexadecoupole parameter β_4 of the nucleus can be obtained from the quadrupole moment Q and hexadecoupole moment H, respectively using the relations

$$\beta_2 = \sqrt{\frac{5\pi}{9}}\frac{Q}{AR^2} \quad \text{and} \quad \beta_4 = \frac{4\pi}{3}\frac{H}{AR^4}, \tag{3}$$

where R is the nuclear radius. The root mean square (rms) matter radius is given as

$$\langle r_m^2\rangle = \frac{1}{A}\int \rho(r_\perp, z).r^2 d\tau. \tag{4}$$

Here, $\rho(r_\perp, z)$ is the deformed density. The total binding energy (BE) and other observables are also obtained by using the standard relations, given in Ref. 21 and 22.

2.1. *Pairing correlations in RMF formalism*

Pairing correlation plays a very crucial role in open shell nuclei. In our calculation, we are using the BCS pairing for determining the bulk properties like BE,

quadrupole deformation parameter and nuclear radii. The pairing energy can be given as:

$$E_{\text{pair}} = -G\left[\sum_{i>0} u_i v_i\right]^2, \tag{5}$$

where G is pairing force constant and v_i^2, $u_i^2 = 1 - v_i^2$ are the occupation probabilities, respectively.[21,30,31] The simple form of BCS equation can be derived from the variational method with respect to the occupation number v_i^2 and is given by:

$$2\epsilon_i u_i v_i - \triangle(u_i^2 - v_i^2) = 0, \tag{6}$$

using $\triangle = G\sum_{i>0} u_i v_i$.

The occupation number is defined as:

$$n_i = v_i^2 = \frac{1}{2}\left[1 - \frac{\epsilon_i - \lambda}{\sqrt{(\epsilon_i - \lambda)^2 + \triangle^2}}\right]. \tag{7}$$

In this calculation, we are dealing with the constant gap formalism for proton and neutron in a region far from beta stability line. These constant gap equation for proton and neutron is taken from Refs. 32 and 33 which is given as:

$$\triangle_p = RB_s e^{sI - tI^2}/Z^{1/3} \tag{8}$$

and

$$\triangle_n = RB_s e^{-sI - tI^2}/A^{1/3} \tag{9}$$

with $R = 5.72$, $s = 0.118$, $t = 8.12$, $B_s = 1$ and $I = (N-Z)/(N+Z)$. In our present calculation, we have taken the constant pairing gap for all states $|\alpha> = |nljm>$ near the Fermi surface for the shake of simplicity. Similar approach was used in the references.[34–36]

As we know, if we go near the neutron drip-line, then coupling to the continuum becomes important.[37–40] In this case, the Relativistic Hartree–Bogoliubov (RHB) approach[41,42] has been proved to be a more accurate formalism for this region. However, in case of RMF-BCS formalism also, the pairing constants along with NL3 parameters are adjusted so that it can reproduce the bulk properties of a nucleus near the drip-line region. For example, in Fig. 1, the total BE/nucleon(A) for Hg isotopes from our calculation is compared with available NL3-RHB data[43] along with existing finite range droplet model (FRDM)[44] and experimental results.[45] The other components of our present calculation like the selection of basis space are described in the next section. It is evident from the figure that the BE from our calculation is in a nice agreement with FRDM and experimental results in neutron rich region. Further, our present result agrees acceptably well with the available RHB data. By using BCS pairing correlation model, it has been shown earlier by different groups[46–50] that the results from RMF BCS (RMF-BCS) approach are almost similar with the RHB formalism. However, due to lack of NL3-RHB data in neutron rich region for the concerned isotopes, we are unable to compare their

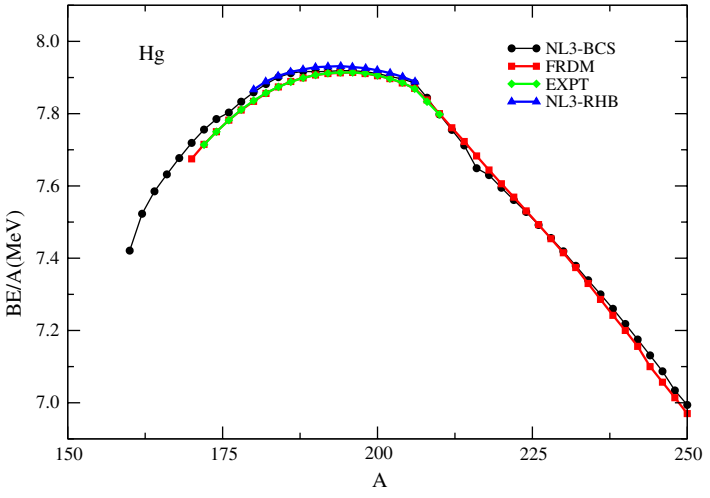

Fig. 1. The BE per particle (BE/A) obtained from RMF(NL3-BCS) (circle) compared with RHB (triangle)[43] FRDM (square)[44] and experimental (diamond)[45] data for Hg isotopes.

individual merits, but the above figure and references suggest that the present formalism can be extended in neutron rich region.

2.2. *Selection of basis space*

In order to choose the proper basis, we calculate the physical observables like BE, rms radii and quadrupole deformation parameter (β_2). To select optimal values for

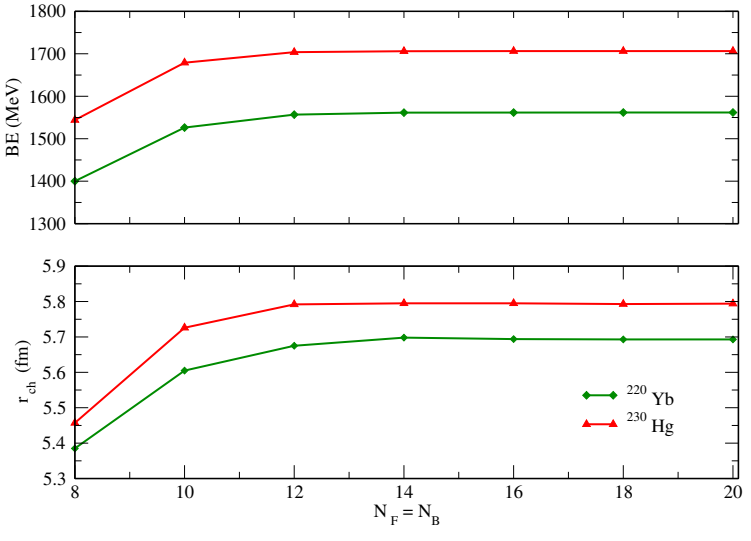

Fig. 2. The variation of calculated BE, charge radii (r_c) with increasing number of Bosonic and Fermionic basis.

N_F and N_B, we select ^{220}Yb and ^{230}Hg as test case and increase the basis quanta from 8 to 20 step by step in Fig. 2. We find that these physical observables vary with changing the bosonic and fermionic oscillator quanta $N_F = N_B = 8$ to 12 but become almost constant after $N_F = N_B = 14$. But our calculation is extended far beyond the stability line which demands a comparatively large basis space for calculation. Therefore, for greater accuracy, we have chosen $N_F = N_B = 20$ for all the calculations. Similar types of calculations are found in Refs. 15, 21 and 51–53.

3. Calculations and Results

RMF model have given very good result in β-stable nuclei of the nuclear landscape. In this work, we are analyzing the exotic neutron drip-line nuclei by using RMF model with well-known NL3[29] parameter set. In 1999, Lalazissis *et al.* [18] analyzed ground state properties of 1315 even–even nuclei with Z between 10 and 98 and calculated total BE, radius and deformations using similar formalism mostly near the stability region. In this paper, we have extended the RMF-BCS formalism near the neutron drip-line for even–even nuclei in $Z = 70-80$ region. In Tables 1–6, the ground state BE, neutron, proton, charge and rms. radius, quadrupole and hexadecoupole parameter of the above isotopes are compared with FRDM[44,54] and experimental data.[45,55,56] In the upcoming subsections, our results are described in detail.

3.1. *Quadrupole deformation*

The Quadrupole deformation parameter β_2 for the ground state for even–even nuclei in $Z = 70-80$ region is determined within the RMF-BCS formalism near the neutron drip-line as an extension of existing data.[18] The parameter β_2 is directly connected to the shape of the nucleus. The ground state quadrupole deformation parameter β_2 is plotted in Fig. 3. We have compared our RMF results with FRDM[54] results.

In case of Yb isotopes in Fig. 3, RMF β_2 data coincides with FRDM[54] values for almost all the mass numbers. In lower mass regions, Yb isotopes are nearly spherical($A = 150$). It changes to oblate at $A = 155$. The prolate stage exists from $A = 160$–190. At $A = 190$–200, it changes from spherical to oblate. At $A = 200$–230 again, it changes to prolate state. In lower and higher mass region, maximum isotopes are prolate in shape. In the middle region, these changes to oblate shape. Therefore one can say that, in Yb isotopes, at $A = 155$ and 190, there is a shape transition from oblate to highly prolate. FRDM also shows the same trend in shapes. The same trend is found in other isotopes except mercury (Hg). Mercury shows prolate shape at $A = 170$–190 whereas FRDM shows oblate shape in the same region.

3.2. *Two-neutron separation energy*

The two-neutron separation energy $S_{2n}(N, Z) = \mathrm{BE}(N, Z) - \mathrm{BE}(N-2, Z)$ is shown in Fig. 4 for Yb, Hf, W, Os, Pt and Hg isotopes. The S_{2n} values calculated

Table 1. The RMF (NL3) results for BE (MeV), Neutron, Proton, Charge, rms radii(fm), quadrupole deformation parameter β_2 and hexadecoupole parameter β_4 for Yb isotopes compared with the FRDM data[44,54] and available experimental results.[45,55,56]

	RMF (NL3)							FRDM			Expt.		
Nucleus	BE(R)	r_n	r_p	$r_{\rm ch}$	$r_{\rm rms}$	β_2	β_4	BE(F)	β_2	β_4	BE(Ex)	$r_{\rm ch}$	β_2
^{150}Yb	1198.1	5.05	5.06	5.12	5.06	−0.15	−0.01	1194.6	−0.16	0.00	1194.6		
^{152}Yb	1220.9	5.06	5.04	5.11	5.05	−0.00	0.00	1218.6	−0.00	0.00	1202.4	5.04	
^{154}Yb	1240.4	5.11	5.06	5.12	5.09	−0.08	0.01	1238.4	−0.01	0.00	1206.0	5.09	
^{156}Yb	1260.3	5.16	5.09	5.15	5.13	0.15	0.05	1257.4	0.13	0.03	1257.6	5.12	
^{158}Yb	1279.1	5.20	5.11	5.18	5.16	0.19	0.06	1276.3	0.16	0.03	1276.5	5.15	0.19
^{160}Yb	1297.0	5.25	5.14	5.2	5.20	0.22	0.06	1294.8	0.21	0.02	1294.8	5.18	0.23
^{162}Yb	1314.3	5.29	5.16	5.22	5.23	0.25	0.08	1312.7	0.23	0.02	1312.6	5.21	0.26
^{164}Yb	1331.4	5.34	5.18	5.25	5.27	0.28	0.11	1330.2	0.26	0.01	1330.0	5.23	0.29
^{166}Yb	1347.8	5.38	5.21	5.27	5.31	0.31	0.11	1347.0	0.27	0.00	1346.7	5.25	0.32
^{168}Yb	1363.6	5.42	5.23	5.29	5.34	0.33	0.10	1363.2	0.28	0.01	1362.8	5.27	0.32
^{170}Yb	1378.6	5.45	5.25	5.31	5.37	0.34	0.07	1378.7	0.30	−0.03	1378.1	5.29	0.33
^{172}Yb	1393.0	5.48	5.26	5.32	5.40	0.34	0.04	1393.3	0.30	−0.04	1392.8	5.30	0.33
^{174}Yb	1406.7	5.51	5.27	5.32	5.42	0.33	0.02	1407.0	0.29	0.02	1406.6	5.31	0.32
^{176}Yb	1419.7	5.54	5.29	5.35	5.44	0.32	−0.00	1420.1	0.28	−0.07	1419.3	5.32	0.31
^{178}Yb	1431.6	5.57	5.30	5.36	5.46	0.31	−0.03	1432.4	0.28	−0.09	1431.6		
^{180}Yb	1443.0	5.60	5.31	5.37	5.49	0.3	−0.06	1443.7	0.28	−0.10	1442.5		
^{182}Yb	1453.7	5.63	5.32	5.38	5.52	0.29	−0.07	1454.3	0.27	−0.11			
^{184}Yb	1462.0	5.66	5.33	5.39	5.54	0.27	−0.08	1464.3	0.26	−0.13			
^{186}Yb	1470.5	5.66	5.32	5.38	5.54	0.21	−0.06	1473.6	0.22	−0.12			
^{188}Yb	1479.4	5.69	5.32	5.38	5.55	−0.20	−0.02	1482.2	0.16	−0.08			
^{190}Yb	1488.0	5.71	5.33	5.39	5.57	−0.18	−0.01	1490.8	−0.19	−0.03			
^{192}Yb	1496.2	5.73	5.33	5.39	5.59	−0.14	−0.02	1499.2	−0.13	−0.03			
^{194}Yb	1505.0	5.75	5.33	5.39	5.60	−0.10	−0.03	1507.8	−0.08	−0.04			
^{196}Yb	1513.0	5.77	5.33	5.39	5.62	0.01	0.00	1516.0	0.01	0.00			
^{198}Yb	1516.7	5.82	5.35	5.41	5.66	0.07	0.02	1520.2	0.02	0.00			
^{200}Yb	1522.0	5.86	5.38	5.44	5.70	0.13	0.08	1523.4	0.06	0.04			
^{202}Yb	1527.4	5.91	5.41	5.47	5.74	0.17	0.10	1527.3	0.11	0.06			
^{204}Yb	1532.1	5.95	5.43	5.49	5.78	0.19	0.09	1531.2	0.14	0.07			
^{206}Yb	1536.5	5.99	5.46	5.51	5.81	0.21	0.08	1535.3	0.16	0.08			
^{208}Yb	1540.4	6.03	5.48	5.53	5.85	0.23	0.08	1539.2	0.18	0.09			
^{210}Yb	1544.9	6.08	5.54	5.60	5.91	0.30	0.20	1542.9	0.21	−0.08			
^{212}Yb	1549.6	6.12	5.56	5.62	5.95	0.32	0.20	1546.2	0.22	0.07			
^{214}Yb	1554.1	6.16	5.59	5.65	5.98	0.34	0.21	1549.3	0.22	0.06			
^{216}Yb	1556.8	6.20	5.6	5.66	6.01	0.34	0.19	1552.4	0.24	0.05			
^{218}Yb	1557.9	6.26	5.65	5.71	6.07	0.40	0.10	1554.8	0.24	0.03			
^{220}Yb	1560.8	6.29	5.67	5.72	6.10	0.40	0.08	1556.8	0.25	−0.01			
^{222}Yb	1564.2	6.29	5.65	5.70	6.09	0.34	0.09	1558.5	0.26	−0.02			
^{224}Yb	1565.9	6.39	5.71	5.76	6.18	0.43	0.12	1559.3	0.26	−0.04			
^{226}Yb	1568.2	6.39	5.69	5.75	6.18	0.39	0.15	1559.9	0.26	−0.06			
^{228}Yb	1569.3	6.43	5.72	5.77	6.22	0.41	0.12	1560.3	0.26	−0.07			
^{230}Yb	1570.2	6.46	5.73	5.79	6.25	0.41	0.11	1560.7	0.26	−0.09			
^{232}Yb	1573.9	6.43	5.66	5.71	6.21	−0.24	−0.02	1560.7	0.25	−0.11			
^{234}Yb	1574.9	6.46	5.67	5.73	6.24	−0.24	−0.03	1559.5	0.23	−0.11			
^{236}Yb	1575.1	6.49	5.68	5.74	6.26	−0.22	−0.04						
^{238}Yb	1575.5	6.51	5.69	5.74	6.28	−0.21	−0.06						
^{240}Yb	1576.2	6.54	5.70	5.75	6.30	−0.19	−0.07						

Table 2. Same as Table 1 for Hf isotopes.

	RMF (NL3)							FRDM			Expt.		
Nucleus	BE(R)	r_n	r_p	$r_{\rm ch}$	$r_{\rm rms}$	β_2	β_4	BE(F)	β_2	β_4	BE(Ex)	$r_{\rm ch}$	β_2
^{152}Hf	1198.8	5.06	5.09	5.15	5.07	−0.13	−0.02	1194.4	−0.15	−0.05			
^{154}Hf	1223.1	5.07	5.08	5.14	5.07	−0.00	0.00	1219.9	0.01	0.00	1219.4		
^{156}Hf	1243.7	5.11	5.09	5.15	5.10	0.07	0.01	1240.8	0.04	−0.01	1240.65		
^{158}Hf	1264.5	5.16	5.12	5.18	5.14	0.14	0.03	1260.8	0.11	0.02	1261.0		
^{160}Hf	1284.3	5.20	5.14	5.20	5.18	0.17	0.03	1280.8	0.15	0.02	1281.0		
^{162}Hf	1303.3	5.25	5.16	5.22	5.21	0.20	0.03	1300.2	0.18	0.01	1300.4		0.16
^{164}Hf	1321.5	5.29	5.18	5.25	5.24	0.23	0.04	1319.0	0.21	0.01	1319.2		0.20
^{166}Hf	1339.4	5.33	5.21	5.27	5.28	0.27	0.08	1337.3	0.23	0.00	1337.4		0.25
^{168}Hf	1357.1	5.38	5.24	5.30	5.32	0.31	0.11	1355.2	0.25	−0.00	1355.0		0.28
^{170}Hf	1374.0	5.42	5.26	5.32	5.35	0.32	0.10	1372.4	0.27	−0.01	1372.0	5.29	0.30
^{172}Hf	1390.1	5.46	5.28	5.34	5.38	0.33	0.08	1388.8	0.28	−0.02	1388.3	5.31	0.28
^{174}Hf	1405.6	5.48	5.29	5.35	5.40	0.32	0.04	1404.6	0.29	−0.04	1403.9	5.32	0.29
^{176}Hf	1420.5	5.51	5.29	5.35	5.42	0.31	0.01	1419.5	0.28	−0.06	1418.8	5.33	0.30
^{178}Hf	1434.6	5.53	5.30	5.36	5.44	0.30	−0.01	1433.8	0.28	−0.08	1432.8	5.34	0.28
^{180}Hf	1447.7	5.56	5.31	5.37	5.47	0.29	−0.04	1447.3	0.28	−0.10	1446.3	5.35	0.27
^{182}Hf	1460.0	5.59	5.33	5.39	5.49	0.28	−0.06	1459.8	0.27	−0.11	1458.7	5.35	
^{184}Hf	1471.6	5.62	5.34	5.40	5.51	0.27	−0.07	1471.6	0.26	−0.13	1470.29		
^{186}Hf	1481.8	5.64	5.34	5.4	5.53	0.24	−0.07	1482.9	0.25	−0.13	1481.3		
^{188}Hf	1492.0	5.66	5.35	5.40	5.54	0.21	−0.07	1493.4	0.21	−0.11	1492.0		
^{190}Hf	1501.8	5.68	5.35	5.41	5.56	0.18	−0.07	1503.2	0.16	−0.08			
^{192}Hf	1510.5	5.71	5.35	5.41	5.58	0.16	−0.06	1512.7	−0.18	−0.03			
^{194}Hf	1519.0	5.72	5.35	5.41	5.59	−0.13	−0.03	1522.3	−0.12	−0.03			
^{196}Hf	1528.9	5.74	5.36	5.42	5.60	−0.09	−0.04	1531.7	−0.08	−0.04			
^{198}Hf	1537.8	5.77	5.36	5.41	5.62	0.00	0.00	1540.7	0.01	0.00			
^{200}Hf	1542.1	5.81	5.38	5.43	5.66	0.06	0.01	1546.0	0.02	0.00			
^{202}Hf	1547.5	5.86	5.41	5.47	5.70	0.12	0.05	1550.1	0.05	0.02			
^{204}Hf	1553.4	5.90	5.43	5.49	5.74	0.16	0.08	1554.5	0.10	0.05			
^{206}Hf	1558.7	5.94	5.46	5.51	5.77	0.18	0.07	1559.2	0.13	0.06			
^{208}Hf	1564.0	5.98	5.48	5.54	5.81	0.20	0.06	1563.7	0.16	0.08			
^{210}Hf	1568.7	6.02	5.50	5.56	5.85	0.22	0.05	1568.4	0.17	0.08			
^{212}Hf	1573.6	6.07	5.56	5.62	5.90	0.29	0.18	1572.8	0.20	0.07			
^{214}Hf	1579.0	6.11	5.58	5.64	5.94	0.31	0.18	1577.0	0.22	0.07			
^{216}Hf	1584.1	6.15	5.61	5.66	5.97	0.33	0.18	1580.8	0.22	0.05			
^{218}Hf	1587.7	6.18	5.62	5.68	6.02	0.33	0.16	1584.4	0.23	0.04			
^{220}Hf	1591.2	6.21	5.64	5.69	6.03	0.33	0.13	1587.6	0.23	0.02			
^{222}Hf	1594.7	6.24	5.66	5.71	6.06	0.33	0.10	1590.7	0.24	−0.00			
^{224}Hf	1597.8	6.27	5.67	5.72	6.09	0.33	0.07	1593.2	0.25	−0.02			
^{226}Hf	1600.8	6.30	5.67	5.73	6.11	0.32	0.03	1594.8	0.24	−0.03			
^{228}Hf	1603.3	6.32	5.68	5.73	6.13	0.31	−0.00	1596	0.23	−0.05			
^{230}Hf	1604.1	6.40	5.72	5.78	6.20	0.22	0.10	1597.5	0.24	−0.08			
^{232}Hf	1607.8	6.37	5.7	5.76	6.17	0.29	−0.05	1598.8	0.24	−0.09			
^{234}Hf	1609.6	6.40	5.71	5.77	6.20	0.28	−0.06	1599.8	0.24	−0.11			
^{236}Hf	1611.4	6.44	5.72	5.77	6.23	0.26	−0.08	1599.4	0.22	−0.11			
^{238}Hf	1613.2	6.47	5.73	5.78	6.25	0.25	−0.09	1598.9	0.22	−0.12			
^{240}Hf	1614.5	6.49	5.74	5.80	6.27	0.25	−0.11	1596.4	0.17	−0.09			
^{242}Hf	1614.7	6.51	5.75	5.80	6.30	0.23	−0.10						

Table 3. Same as Table 1 for W isotopes.

	RMF (NL3)							FRDM			Expt.		
Nucleus	BE(R)	r_n	r_p	$r_{\rm ch}$	$r_{\rm rms}$	β_2	β_4	BE(F)	β_2	β_4	BE(Ex)	$r_{\rm ch}$	β_2
^{154}W	1198.0	5.06	5.12	5.18	5.09	−0.11	−0.02	1192.8	−0.12	−0.04			
^{156}W	1224.1	5.08	5.11	5.17	5.09	−0.01	0.0	1219.4	0.01	0.00			
^{158}W	1245.6	5.12	5.12	5.19	5.12	−0.04	0.00	1241.7	0.02	0.00	1241.1		
^{160}W	1267.1	5.16	5.15	5.21	5.16	0.11	0.01	1262.6	0.09	0.00	1262.9		
^{162}W	1287.9	5.20	5.17	5.23	5.19	0.15	0.01	1283.5	0.13	0.02	1283.7		
^{164}W	1307.7	5.25	5.19	5.25	5.22	0.17	0.01	1303.9	0.16	0.01	1304.0		
^{166}W	1326.6	5.29	5.21	5.27	5.25	0.20	0.02	1323.7	0.18	−0.00	1323.8		
^{168}W	1345.4	5.35	5.25	5.31	5.31	0.28	0.02	1342.9	0.21	0.00	1343.0		0.23
^{170}W	1364.5	5.39	5.28	5.34	5.34	0.32	0.12	1361.6	0.23	−0.01	1361.5		0.24
^{172}W	1382.6	5.43	5.30	5.36	5.37	0.33	0.11	1379.7	0.25	−0.00	1379.5		0.28
^{174}W	1399.7	5.46	5.31	5.37	5.40	0.33	0.09	1397.1	0.27	−0.01	1396.7		0.25
^{176}W	1416.1	5.49	5.32	5.38	5.42	0.33	0.06	1413.8	0.27	−0.03	1413.3		
^{178}W	1431.9	5.51	5.33	5.39	5.44	0.31	0.02	1429.9	0.27	−0.05	1429.2		
^{180}W	1447.0	5.54	5.33	5.39	5.45	0.29	−0.01	1445.4	0.26	−0.07	1444.6	5.35	0.25
^{182}W	1461.2	5.56	5.34	5.40	5.47	0.28	−0.04	1459.9	0.26	−0.08	1459.3	5.36	0.25
^{184}W	1474.7	5.59	5.35	5.41	5.49	0.26	−0.06	1473.6	0.24	−0.10	1472.9	5.37	0.24
^{186}W	1487.4	5.62	5.36	5.42	5.52	0.25	−0.08	1486.7	0.23	−0.11	1485.9	5.37	0.23
^{188}W	1499.3	5.64	5.36	5.42	5.53	0.22	−0.08	1499.1	0.21	−0.11	1498.2		
^{190}W	1510.9	5.65	5.37	5.43	5.54	0.20	−0.08	1510.8	0.17	−0.10	1509.9		
^{192}W	1521.8	5.68	5.37	5.43	5.56	0.17	−0.08	1522.28	0.16	−0.08	1521.41		
^{194}W	1531.4	5.70	5.38	5.43	5.58	0.15	−0.07	1532.5	−0.17	−0.03			
^{196}W	1540.8	5.72	5.38	5.43	5.59	0.11	−0.05	1543.3	−0.11	−0.03			
^{198}W	1551.4	5.74	5.38	5.44	5.61	−0.08	−0.04	1553.8	−0.07	−0.04			
^{200}W	1561.6	5.76	5.38	5.44	5.62	0.00	0.00	1563.7	0.01	0.00			
^{202}W	1566.2	5.80	5.40	5.46	5.66	0.03	0.00	1570.0	0.01	0.00			
^{204}W	1571.8	5.84	5.43	5.48	5.70	0.10	0.03	1575.1	0.04	0.01			
^{206}W	1577.9	5.89	5.45	5.51	5.73	0.14	0.06	1580.0	0.08	0.04			
^{208}W	1583.7	5.93	5.47	5.53	5.77	0.16	0.06	1585.2	0.11	0.05			
^{210}W	1589.4	5.97	5.49	5.55	5.80	0.18	0.05	1590.4	0.14	0.06			
^{212}W	1594.3	6.02	5.55	5.61	5.86	0.26	0.14	1595.7	0.16	0.07			
^{214}W	1600.9	6.06	5.58	5.64	5.90	0.29	0.16	1600.8	0.18	0.07			
^{216}W	1606.9	6.10	5.60	5.66	5.94	0.31	0.16	1605.7	0.21	0.07			
^{218}W	1612.7	6.14	5.62	5.68	5.97	0.32	0.16	1610.3	0.22	0.04			
^{220}W	1617.3	6.17	5.64	5.70	6.00	0.32	0.14	1614.6	0.22	0.03			
^{222}W	1621.9	6.20	5.66	5.71	6.02	0.32	0.11	1618.6	0.23	0.00			
^{224}W	1626.2	6.23	5.68	5.73	6.05	0.33	0.09	1622.2	0.23	−0.01			
^{226}W	1629.9	6.26	5.69	5.75	6.08	0.33	0.07	1625.4	0.23	−0.03			
^{228}W	1633.5	6.30	5.70	5.76	6.11	0.33	0.04	1627.8	0.22	−0.04			
^{230}W	1636.3	6.32	5.72	5.77	6.14	0.33	0.02	1630.1	0.22	−0.06			
^{232}W	1638.8	6.35	5.73	5.79	6.16	0.32	−0.00	1632.4	0.22	−0.07			
^{234}W	1641.3	6.37	5.74	5.80	6.18	0.30	−0.03	1634.5	0.22	−0.08			
^{236}W	1643.3	6.40	5.75	5.80	6.20	0.28	−0.05	1636.3	0.22	−0.10			
^{238}W	1645.5	6.42	5.75	5.80	6.22	0.26	−0.08	1636.9	0.21	−0.11			
^{240}W	1648.1	6.45	5.76	5.81	6.24	0.25	−0.10	1636.9	0.19	−0.10			
^{242}W	1650.5	6.47	5.77	5.83	6.27	0.24	−0.12	1635.9	0.16	−0.09			
^{244}W	1651.1	6.50	5.77	5.83	6.29	0.22	−0.11	1636.2	0.16	−0.10			

Table 4. Same as Table 1 for Os isotopes.

	RMF (NL3)							FRDM			Expt.		
Nucleus	BE(R)	r_n	r_p	$r_{\rm ch}$	$r_{\rm rms}$	β_2	β_4	BE(F)	β_2	β_4	BE(Ex)	$r_{\rm ch}$	β_2
^{156}Os	1195.9	5.06	5.15	5.21	5.10	−0.08	−0.02						
^{158}Os	1223.8	5.08	5.14	5.21	5.11	−0.00	0.00						
^{160}Os	1246.4	5.12	5.16	5.22	5.14	−0.00	0.00	1241.0	0.01				
^{162}Os	1287.9	5.20	5.17	5.23	5.19	0.15	0.00	1262.8	0.05	−0.01	1262.6		
^{164}Os	1307.7	5.25	5.19	5.25	5.22	0.17	0.00	1284.5	0.11	−0.00	1284.7		
^{166}Os	1310.3	5.24	5.21	5.27	5.23	0.13	−0.00	1305.8	0.13	−0.00	1305.8		
^{168}Os	1330.0	5.28	5.23	5.29	5.26	0.16	0.00	1326.6	0.16	−0.01	1326.5		
^{170}Os	1349.3	5.35	5.28	5.34	5.32	0.27	0.10	1346.7	0.17	−0.01	1346.6		
^{172}Os	1382.5	5.43	5.30	5.36	5.37	0.33	0.11	1366.3	0.19	−0.01	1366.05		0.23
^{174}Os	1388.5	5.43	5.33	5.39	5.39	0.32	0.10	1385.3	0.23	−0.01	1384.9		0.27
^{176}Os	1416.9	5.49	5.32	5.38	5.42	0.33	0.08	1403.6	0.25	−0.01	1403.2		
^{178}Os	1424.3	5.50	5.36	5.42	5.44	0.33	0.06	1421.3	0.25	−0.03	1420.8		
^{180}Os	1441.4	5.52	5.37	5.43	5.46	0.32	0.03	1438.5	0.24	−0.05	1437.7		0.23
^{182}Os	1461.2	5.56	5.34	5.40	5.47	0.28	0.00	1454.9	0.24	−0.06	1454.1		0.23
^{184}Os	1472.3	5.57	5.38	5.44	5.49	0.29	−0.03	1470.7	0.23	−0.07	1469.9	5.38	0.21
^{186}Os	1487.4	5.62	5.36	5.42	5.52	0.25	−0.05	1485.4	0.22	−0.08	1484.8	5.39	0.20
^{188}Os	1500.0	5.62	5.39	5.45	5.53	0.24	−0.07	1499.3	0.19	−0.09	1499.1	5.40	0.19
^{190}Os	1512.9	5.63	5.38	5.44	5.53	0.20	−0.07	1512.8	0.16	−0.08	1512.8	5.41	0.18
^{192}Os	1526.1	5.65	5.38	5.44	5.54	0.18	−0.07	1526.3	0.16	−0.08	1526.1	5.41	0.17
^{194}Os	1531.4	5.70	5.37	5.43	5.58	0.15	−0.07	1539.0	0.15	−0.08	1538.8		
^{196}Os	1549.6	5.69	5.39	5.45	5.57	0.12	−0.06	1550.5	−0.16	−0.03	1550.8		
^{198}Os	1551.4	5.74	5.38	5.44	5.61	−0.10	−0.04	1562.6	−0.10	−0.03			
^{200}Os	1572.6	5.73	5.40	5.46	5.61	−0.06	−0.03	1574.1	−0.06	−0.04			
^{202}Os	1584.1	5.76	5.40	5.46	5.63	0.00	−0.00	1584.9	0.01	0.00			
^{204}Os	1589.6	5.80	5.42	5.48	5.66	0.00	−0.00	1592.0	0.01	0.00			
^{206}Os	1594.8	5.83	5.44	5.50	5.69	0.07	0.01	1598.0	0.03	0.01			
^{208}Os	1583.7	5.93	5.47	5.53	5.77	0.16	0.04	1603.7	0.05	0.02			
^{210}Os	1607.4	5.91	5.49	5.55	5.76	0.14	0.05	1609.5	0.10	0.04			
^{212}Os	1613.4	5.95	5.51	5.57	5.80	0.16	0.05	1615.4	0.12	0.05			
^{214}Os	1600.9	6.06	5.58	5.64	5.90	0.29	0.13	1621.1	0.15	0.05			
^{216}Os	1625.6	6.05	5.60	5.65	5.89	0.27	0.15	1627.0	0.17	0.06			
^{218}Os	1632.2	6.09	5.63	5.68	5.93	0.30	0.15	1632.5	0.20	0.06			
^{220}Os	1638.9	6.13	5.65	5.71	5.97	0.32	0.15	1637.9	0.21	0.05			
^{222}Os	1644.6	6.16	5.67	5.73	6.00	0.33	0.13	1642.9	0.21	0.03			
^{224}Os	1650.0	6.19	5.69	5.75	6.02	0.33	0.10	1647.7	0.22	0.02			
^{226}Os	1655.3	6.22	5.71	5.77	6.06	0.34	0.09	1652.0	0.22	0.00			
^{228}Os	1659.7	6.26	5.72	5.78	6.09	0.34	0.02	1656.0	0.23	−0.02			
^{230}Os	1663.8	6.29	5.74	5.79	6.09	0.34	0.04	1659.2	0.22	−0.03			
^{232}Os	1667.6	6.32	7.76	5.81	6.14	0.33	0.02	1662.2	0.21	−0.05			
^{234}Os	1670.6	6.34	5.77	5.82	6.16	0.32	−0.00	1665.1	0.20	−0.06			
^{236}Os	1673.5	6.36	5.77	5.83	6.18	0.31	−0.02	1668.0	0.20	−0.07			
^{238}Os	1675.8	6.39	5.78	5.83	6.20	0.29	−0.05	1670.5	0.21	−0.09			
^{240}Os	1678.4	6.42	5.78	5.84	6.22	0.27	−0.07	1671.7	0.18	−0.09			
^{242}Os	1681.1	6.44	5.79	5.85	6.24	0.26	−0.09	1671.9	0.16	−0.08			
^{244}Os	1683.8	6.47	5.80	5.86	6.27	0.25	−0.11	1672.6	0.16	−0.07			
^{246}Os	1684.5	6.49	5.81	5.86	6.29	0.23	−0.10	1671.2	0.11	−0.03			

Table 5. Same as Table 1 for Pt isotopes.

	RMF (NL3)							FRDM			Expt.		
Nucleus	BE(R)	r_n	r_p	$r_{\rm ch}$	$r_{\rm rms}$	β_2	β_4	BE(F)	β_2	β_4	BE(Ex)	$r_{\rm ch}$	β_2
^{158}Pt	1192.2	5.06	5.18	5.24	5.12	−0.00	0.00						
^{160}Pt	1222.1	5.09	5.18	5.24	5.13	−0.002	0.00						
^{162}Pt	1246.0	5.13	5.19	5.25	5.16	−0.00	0.00						
^{164}Pt	1268.2	5.16	5.20	5.27	5.18	−0.03	0.00						
^{166}Pt	1290.3	5.20	5.22	5.28	5.21	0.07	0.00	1283.8	−0.07	−0.01	1283.7		
^{168}Pt	1310.0	5.24	5.24	5.30	5.24	0.08	−0.00	1305.6	−0.10	−0.01	1306.0		
^{170}Pt	1332.0	5.28	5.25	5.31	5.26	0.09	−0.01	1327.2	0.11	−0.00	1327.4		
^{172}Pt	1351.3	5.35	5.30	5.36	5.33	0.25	0.09	1348.2	0.13	−0.01	1348.3		
^{174}Pt	1372.2	5.40	5.33	5.39	5.33	0.29	0.11	1368.7	0.15	−0.01	1368.7		
^{176}Pt	1392.3	5.44	5.36	5.41	5.40	0.31	0.10	1388.5	0.17	−0.01	1388.5		0.19
^{178}Pt	1411.7	5.47	5.37	5.43	5.43	0.32	0.08	1407.9	0.25	0.01	1407.7	5.37	
^{180}Pt	1430.6	5.50	5.39	5.45	5.45	0.32	0.05	1426.4	0.27	−0.01	1426.2	5.39	0.26
^{182}Pt	1448.8	5.53	5.40	5.46	5.48	0.32	0.03	1444.4	0.26	−0.03	1444.1	5.40	
^{184}Pt	1465.7	5.56	5.41	5.47	5.50	0.31	0.01	1461.9	0.25	−0.04	1461.4	5.40	0.22
^{186}Pt	1481.6	5.58	5.42	5.48	5.51	0.30	−0.01	1478.5	0.24	−0.06	1478.1	5.40	0.20
^{188}Pt	1496.2	5.61	5.42	5.48	5.53	0.28	−0.03	1493.5	−0.16	−0.01	1494.2	5.41	0.19
^{190}Pt	1510.0	5.63	5.42	5.48	5.54	0.25	−0.05	1509.1	−0.16	−0.02	1509.9	5.41	0.15
^{192}Pt	1524.3	5.62	5.40	5.46	5.53	0.18	−0.06	1524.2	−0.16	−0.03	1525.0	5.42	0.15
^{194}Pt	1538.9	5.64	5.40	5.45	5.54	0.14	−0.06	1539.0	−0.15	−0.03	1539.6	5.42	0.14
^{196}Pt	1552.8	5.66	5.40	5.46	5.55	−0.13	−0.03	1553.2	−0.14	−0.03	1553.6	5.43	0.13
^{198}Pt	1566.3	5.68	5.40	5.46	5.46	−0.11	−0.02	1566.8	−0.14	−0.03	1567.0	5.44	0.11
^{200}Pt	1579.6	5.70	5.41	5.47	5.59	−0.08	−0.03	1580.0	−0.09	−0.03	1579.9		
^{202}Pt	1592.5	5.72	5.42	5.47	5.61	−0.00	0.00	1592.5	−0.06	−0.04			
^{204}Pt	1605.3	5.75	5.42	5.48	5.63	0.00	0.00	1604.1	0.01	0.00			
^{206}Pt	1611.6	5.79	5.44	5.5	5.66	0.00	0.00	1612.1	0.01	0.00			
^{208}Pt	1617.1	5.83	5.46	5.52	5.69	−0.04	0.01	1618.9	0.03	0.00			
^{210}Pt	1615.2	6.00	5.65	5.70	5.87	0.09	0.12	1625.5	0.05	0.01			
^{212}Pt	1623.7	6.04	5.67	5.73	5.91	0.14	0.12	1631.9	0.08	0.03			
^{214}Pt	1635.8	5.94	5.53	5.58	5.79	0.13	0.05	1638.4	0.11	0.04			
^{216}Pt	1641.7	6.00	5.58	5.64	5.85	0.22	0.12	1644.9	0.13	0.05			
^{218}Pt	1649.0	6.04	5.61	5.67	5.89	0.25	0.14	1651.2	0.16	0.07			
^{220}Pt	1656.1	6.08	5.64	5.70	5.93	0.29	0.14	1657.4	0.19	0.07			
^{222}Pt	1663.3	6.12	5.67	5.73	5.97	0.31	0.14	1663.4	0.20	0.06			
^{224}Pt	1669.8	6.15	5.69	5.75	6.00	0.31	0.11	1669.2	0.21	0.05			
^{226}Pt	1676.1	6.18	5.71	5.77	6.02	0.32	0.09	1674.6	0.22	0.03			
^{228}Pt	1682.2	6.21	5.73	5.78	6.05	0.32	0.07	1679.7	0.22	0.02			
^{230}Pt	1687.0	6.25	5.74	5.80	6.08	0.32	0.05	1684.3	0.23	−0.00			
^{232}Pt	1691.7	6.28	5.76	5.81	6.11	0.33	0.02	1688.2	0.21	−0.02			
^{234}Pt	1696.3	6.31	5.78	5.83	6.14	0.33	0.00	1691.8	0.19	−0.03			
^{236}Pt	1700.4	6.33	5.79	5.84	6.16	0.31	−0.01	1695.2	0.18	−0.04			
^{238}Pt	1704.3	6.35	5.80	5.86	6.18	0.30	−0.03	1698.8	0.18	−0.05			
^{240}Pt	1707.3	6.38	5.81	5.87	6.20	0.29	−0.05	1702.1	0.19	−0.08			
^{242}Pt	1710.2	6.41	5.82	5.88	6.23	0.28	−0.07	1704.1	0.17	−0.09			
^{244}Pt	1713.2	6.44	5.83	5.89	6.25	0.27	−0.08	1705.3	0.16	−0.06			
^{246}Pt	1716.2	6.47	5.84	5.90	6.28	0.26	−0.10	1705.7	0.10	−0.03			
^{248}Pt	1716.7	6.46	5.77	5.83	6.25	−0.15	−0.08	1706.8	0.09	−0.01			

Table 6. Same as Table 1 for Hg isotopes.

	RMF (NL3)							FRDM			Expt.		
Nucleus	BE(R)	r_n	r_p	$r_{\rm ch}$	$r_{\rm rms}$	β_2	β_4	BE(F)	β_2	β_4	BE(Ex)	$r_{\rm ch}$	β_2
^{160}Hg	1187.3	5.07	5.22	5.28	5.15	−0.00	0.00						
^{162}Hg	1218.7	5.10	5.22	5.28	5.16	−0.00	0.00						
^{164}Hg	1243.9	5.13	5.22	5.29	5.18	−0.00	0.00						
^{166}Hg	1267.0	5.17	5.24	5.30	5.20	−0.00	0.00						
^{168}Hg	1289.7	5.21	5.25	5.31	5.23	−0.01	0.00						
^{170}Hg	1312.2	5.24	5.27	5.33	5.25	−0.00	0.00	1304.7	−0.08	−0.01			
^{172}Hg	1334.0	5.27	5.28	5.34	5.28	−0.00	0.00	1326.9	−0.10	−0.02	1326.8		
^{174}Hg	1354.6	5.31	5.29	5.35	5.3	0.00	0.00	1348.5	−0.11	−0.03	1348.5		
^{176}Hg	1373.3	5.40	5.36	5.42	5.38	0.27	0.11	1369.6	−0.11	−0.03	1369.7		
^{178}Hg	1394.3	5.44	5.38	5.44	5.41	0.30	0.10	1390.1	−0.11	−0.03	1390.4		
^{180}Hg	1414.7	5.47	5.40	5.46	5.44	0.31	0.08	1410.2	−0.12	−0.03	1410.5		
^{182}Hg	1434.5	5.51	5.41	5.47	5.47	0.31	0.06	1429.8	−0.12	−0.02	1430.0	5.38	
^{184}Hg	1453.7	5.54	5.43	5.48	5.49	0.31	0.03	1448.9	−0.13	−0.02	1448.9	5.39	0.16
^{186}Hg	1471.6	5.56	5.44	5.49	5.51	0.31	0.01	1467.3	−0.13	−0.03	1467.2	5.40	0.13
^{188}Hg	1488.4	5.59	5.44	5.50	5.53	0.30	−0.01	1485.1	−0.13	−0.03	1485.0	5.41	
^{190}Hg	1504.1	5.61	5.45	5.51	5.55	0.28	−0.03	1502.3	−0.13	−0.03	1502.3	5.42	
^{192}Hg	1520.1	5.59	5.40	5.46	5.51	−0.15	−0.02	1519	−0.13	−0.03	1519.1	5.42	
^{194}Hg	1536.3	5.61	5.41	5.46	5.53	−0.14	−0.03	1535.2	−0.13	−0.04	1535.4	5.43	
^{196}Hg	1552.1	5.63	5.41	5.47	5.55	−0.14	−0.03	1551.1	−0.12	−0.03	1551.2	5.44	0.12
^{198}Hg	1567.4	5.66	5.42	5.48	5.56	−0.12	−0.02	1566.3	−0.12	−0.03	1566.5	5.45	0.11
^{200}Hg	1582.1	5.68	5.42	5.48	5.58	−0.09	−0.02	1581.0	−0.11	−0.03	1581.2	5.46	0.10
^{202}Hg	1596.4	5.70	5.43	5.49	5.59	−0.00	0.00	1595.1	−0.09	−0.04	1595.2	5.46	0.08
^{204}Hg	1610.8	5.72	5.44	5.49	5.59	0.00	0.00	1608.6	−0.06	−0.04	1608.7	5.47	0.07
^{206}Hg	1624.3	5.75	5.44	5.50	5.63	0.00	0.00	1621.3	−0.01	0.00	1621.0	5.48	
^{208}Hg	1631.6	5.79	5.46	5.52	5.67	0.00	0.00	1630.3	−0.01	0.01	1629.3		
^{210}Hg	1637.5	5.82	5.48	5.54	5.70	−0.00	0.00	1638.0	−0.03	−0.01	1637.6		
^{212}Hg	1644.0	5.86	5.51	5.56	5.73	−0.05	0.00	1645.4	−0.04	−0.01			
^{214}Hg	1650.4	5.89	5.53	5.59	5.76	−0.06	−0.00	1652.7	−0.05	−0.01			
^{216}Hg	1652.1	6.09	5.74	5.80	5.96	0.12	0.15	1659.5	−0.08	−0.01			
^{218}Hg	1663.2	5.98	5.59	5.65	5.84	0.19	0.12	1666.3	−0.09	−0.01			
^{220}Hg	1670.8	6.03	5.62	5.68	5.88	0.23	0.14	1673.3	0.16	0.08			
^{222}Hg	1678.6	6.07	5.66	5.71	5.92	0.27	0.14	1680.3	0.19	0.08			
^{224}Hg	1686.2	6.11	5.68	5.74	5.96	0.29	0.13	1687.0	0.20	0.06			
^{226}Hg	1693.2	6.14	5.70	5.76	5.99	0.30	0.11	1693.5	0.21	0.06			
^{228}Hg	1700.0	6.17	5.72	5.78	6.02	0.30	0.09	1699.6	0.22	0.04			
^{230}Hg	1706.4	6.20	5.74	5.79	6.04	0.31	0.07	1705.4	0.22	0.03			
^{232}Hg	1711.8	6.23	5.76	5.81	6.07	0.31	0.05	1710.7	0.23	0.01			
^{234}Hg	1717.3	6.27	5.78	5.84	6.11	0.32	0.02	1715.2	0.22	−0.01			
^{236}Hg	1722.8	6.30	5.80	5.86	6.14	0.32	−0.10	1719.5	0.20	−0.02			
^{238}Hg	1727.8	6.32	5.82	5.87	6.16	0.31	−0.03	1723.7	0.19	−0.04			
^{240}Hg	1732.4	6.35	5.83	5.88	6.18	0.30	−0.04	1728.0	0.19	−0.05			
^{242}Hg	1736.4	6.37	5.84	5.90	6.20	0.29	−0.06	1731.7	0.20	−0.07			
^{244}Hg	1739.9	6.40	5.85	5.91	6.23	0.28	−0.08	1732.5	−0.06	0.00			
^{246}Hg	1743.3	6.43	5.86	5.92	6.25	0.27	−0.09	1736.0	−0.07	0.00			
^{248}Hg	1744.5	6.42	5.79	5.85	6.23	−0.18	−0.04	1739.5	−0.09	−0.01			
^{250}Hg	1748.5	6.45	5.79	5.85	6.24	−0.16	−0.06	1742.4	−0.10	0.00			

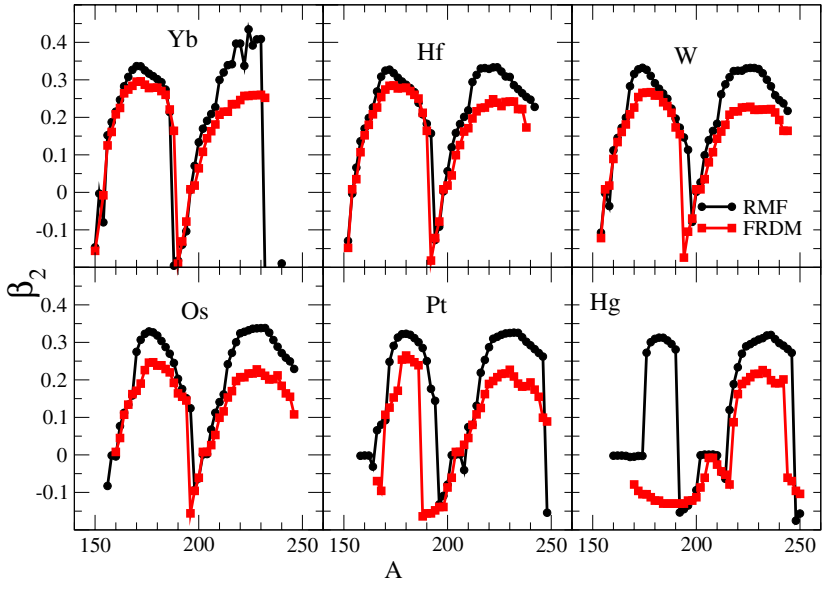

Fig. 3. The quadrupole moment deformation parameter β_2 obtained from RMF(NL3)(circle) compared with the FRDM (square)[54] results for different isotopes of Yb, Hf, W, Os, Pt and Hg in $Z = 70-80$ drip-line region.

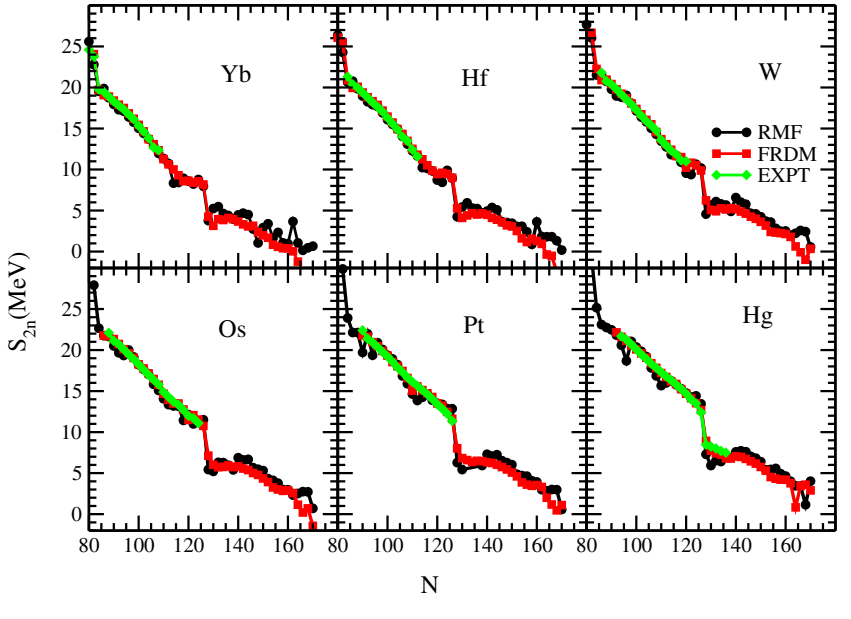

Fig. 4. Two-neutron separation energy S_{2n} (RMF)(circle) is compared with FRDM (square) and experimental results (diamond) for different isotopes of $Z = 70-80$ region.

from RMF, FRDM[44] and Experimental[45] results are compared in Fig. 4. We can predict the stability of these nuclei by S_{2n} energy. If S_{2n} is large, it means nuclei will be stable with two-neutron separation whereas the two-neutron drip-line for an isotopic chain can be identified as the nucleus having zero or slightly positive separation energy value. Therefore, it is evident from the figure that the two-neutron drip-line for the $Z = 70$(Yb) isotope comes at $N = 166$, the same for $Z = 72, 74, 76$ isotopes is approximately at $N = 170$. In case of $Z = 80$(Hg), the two-neutron drip-line arrives at the neutron number $N = 168$. Furthermore, in all cases, the S_{2n} values decrease gradually with increase in neutron number. There is a kink appeared at neutron magic number $N = 126$ in every case. In order to visualize this scenario with a bit clarity, in the next subsection, we defined differential variation of two-neutron separation energy given in Fig. 5.

3.3. *Differential variation of two-neutron separation energy*

The differential variation of the two-neutron separation energy S_{2n} with respect to the neutron number(N), i.e., $dS_{2n}(Z, N)$ is defined as:

$$dS_{2n}(Z, N) = \frac{S_{2n}(Z, N + 2) - S_{2n}(Z, N)}{2}. \tag{10}$$

The $dS_{2n}(Z, N)$ is an important factor to find the rate of change of separation energy with respect to the neutron number in an isotopic chain. Here, we calculated the $dS_{2n}(Z, N)$ for NL3 parameters and compared it with FRDM and experimental

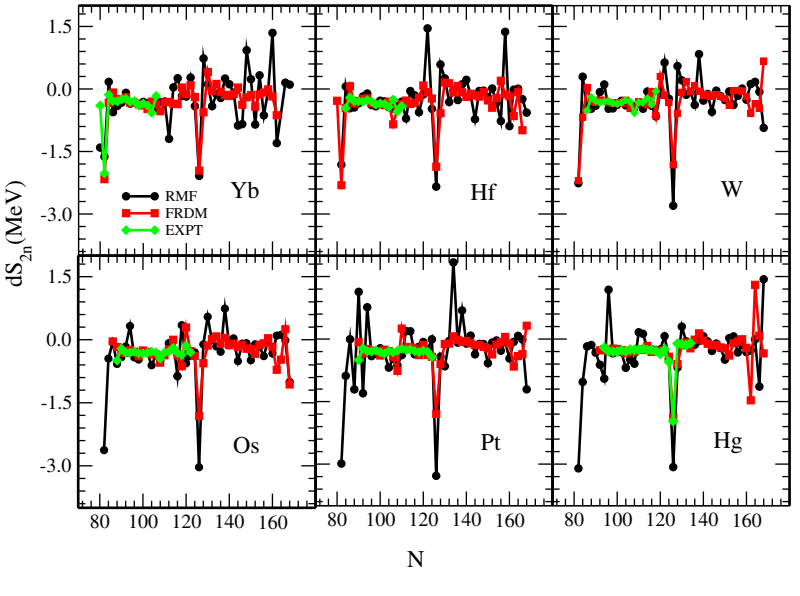

Fig. 5. The differential variation of two-neutron separation energy dS_{2n} (RMF)(circle) is compared with FRDM (square) and experimental results (diamond) for different isotopes of $Z = 70-80$ region.

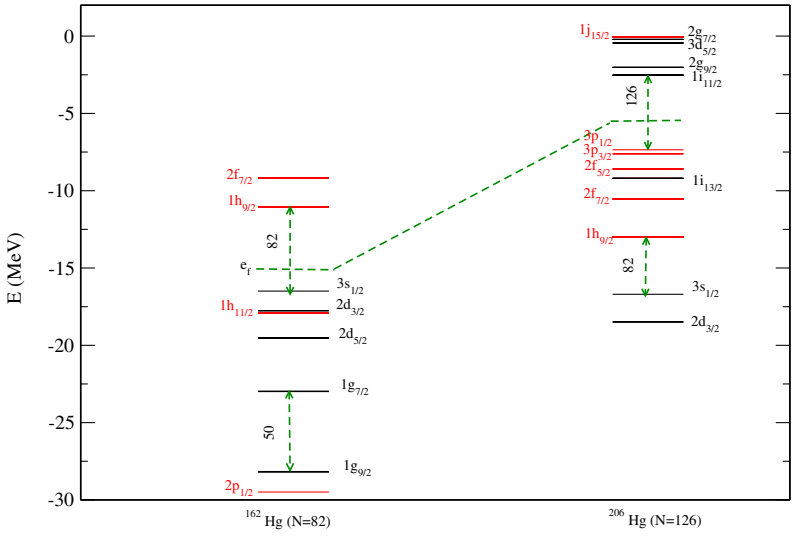

Fig. 6. The single particle energy levels for ^{162}Hg and ^{206}Hg isotopes from RMF model with NL3 parameter set. The dashed-line indicate the fermi surface e_f.

results extracted from Refs. 44 and 45, respectively. In general, the large, sharp, deep fall in the $dS_{2n}(Z,N)$ is observed for Yb, Hf, W, Os, Pt and Hg isotopes at $N = 82$ and 126 (Fig. 5). It shows the neutron shell closures at $N = 82$ and $N = 126$.

3.4. *Single Particle energy levels*

In Fig. 6, we plotted single particle energies for neutron levels near the Fermi surface for Hg isotopes ($Z = 80$) at neutron shell closures ($N = 82$ and 126). We have used deformed configuration to calculate these levels. From Table 6, it is evident that ^{162}Hg and ^{206}Hg are nearly spherical and therefore the single particle levels are almost identical to that of the spherical configuration. For example, in ^{162}Hg, the level $g_{7/2}$ actually consists of four overlapped energy states having spins $7/2^+, 5/2^+, 3/2^+$ and $1/2^+$. In both cases, we found some large gaps at $N = 50, 82, 126$ shell closures. Here, the green dotted line shows the approximate fermi level. In case of Yb, Hf, W, Os and Pt also the gaps are visible at magic shell closures. However, they are not depicted in this paper.

4. Decay Modes

In this section, we discuss probable decay modes of these neutron-rich nuclei.

4.1. *Alpha decay half-life*

The Q_α energy is obtained from the relation[57]: $Q_\alpha(N,Z) = BE(N,Z) — BE(N-2, Z-2) — BE(2,2)$. Here, $BE(N,Z)$ is the BE of the parent nucleus with neutron

number N and proton number Z, $BE(2,2)$ is the BE of the α-particle (^{4}He), i.e., 28.296 MeV, and $BE(N-2, Z-2)$ is the BE of the daughter nucleus after the emission of an α-particle.

The expression for the α-decay half-life from Viola and Seaborg[58] is given by:

$$\log_{10} T^{\alpha}_{1/2}(s) = \frac{aZ-b}{\sqrt{Q_\alpha}} - (cZ+d) + h_{\log} \tag{11}$$

with Z as the number of proton for the parent nucleus and the constants a, b, c and d, are from Sobiczewski *et al.*[59] The values of these constants are $a = 1.66175$, $b = 8.5166$, $c = 0.20228$, $d = 33.9069$ and the quantity $h_{\log}$ accounts for the hindrances associated with the odd nucleon as,

$$\begin{aligned} h_{\log} &= 0 && \text{for } Z \text{ even and } N \text{ even} \\ &= 0.772 && \text{for } Z \text{ odd and } N \text{ even} \\ &= 1.066 && \text{for } Z \text{ even and } N \text{ odd} \\ &= 1.114 && \text{for } Z \text{ odd and } N \text{ odd.} \end{aligned} \tag{12}$$

We evaluate the BE by using RMF formalism and from these, we estimated the Q_α for all the isotopes of $Z = 70-80$ region. We have calculated the half-life time $T^{\alpha}_{1/2}$ by using the above formulae. The comparison of Q_α and $T^{\alpha}_{1/2}$ is shown in Figs. 7 and 8, respectively. From Fig. 8, it is evident that the alpha decay half-life goes on increasing with large neutron numbers and follows a similar trend for RMF,

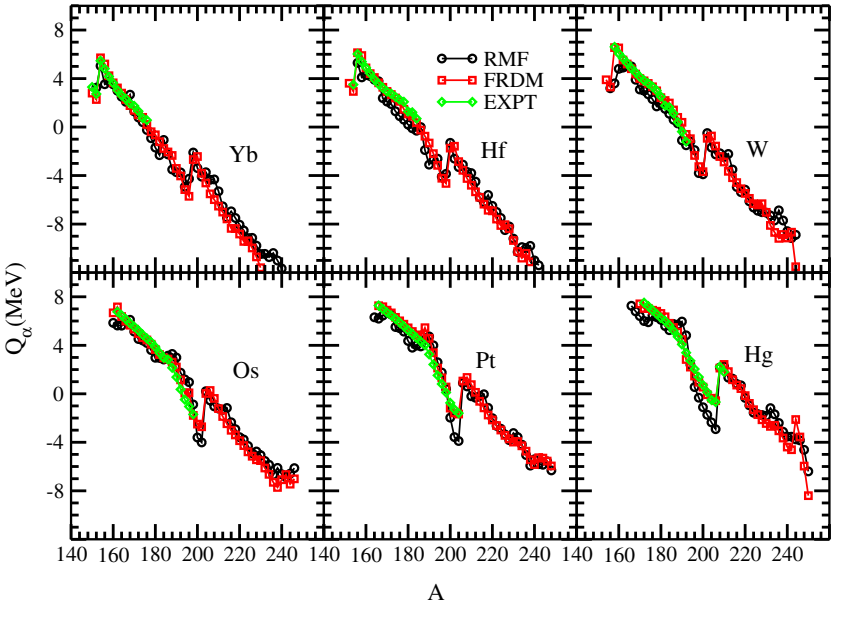

Fig. 7. The Q_α energy obtained from RMF(NL3)(circle) compared with the FRDM(square) and experimental(diamond) results for different isotopes of $Z = 70-80$ region.

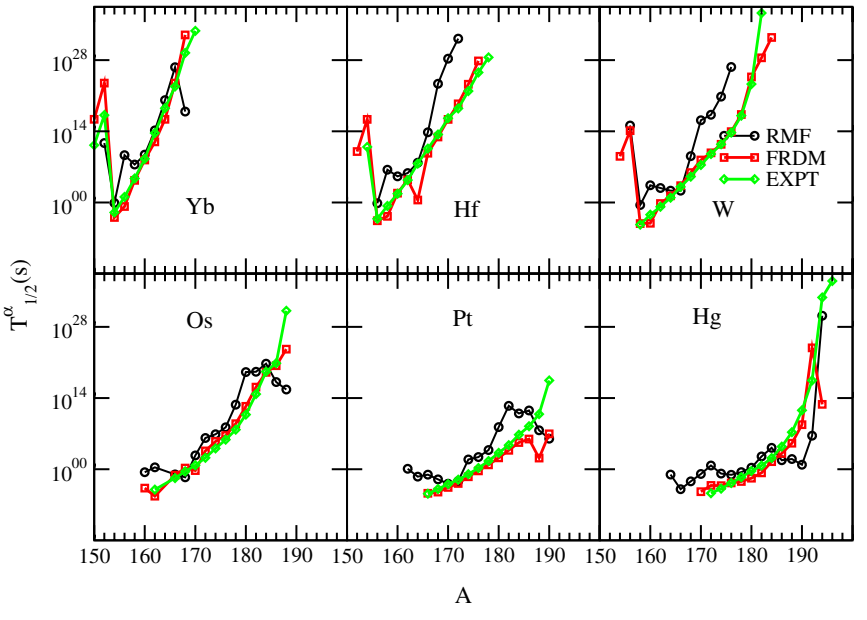

Fig. 8. The $T^{\alpha}_{1/2}$ obtained from RMF(NL3)(circle) are compared with FRDM(square) and experimental(diamond) results in $Z = 70$–80 region.

FRDM and experimental cases. In another word, we can say that these neutron rich nuclei hardly exhibit α-decay and therefore the concerned decay channel is almost forbidden in this region.

In order to check the usual decay mechanism of these neutron-rich samples, in the next subsection, we studied the β decay half-life.

4.2. *Beta decay half-life*

As discussed in the previous subsection, we expect β decay to be the prominent mode in case of neutron-rich nuclei. In order to calculate β decay half-life, we have used the empirical formula of Fiset and Nix.[60] However, the formula holds good mainly for the superheavy region, but in this work we have checked its credibility in $Z = 70-80$ region. The formula for β decay half-life is defined as:

$$T^{\beta}_{1/2} = (540 \times 10^5)\frac{{m_e}^5}{\rho_{\text{d.s.}}({W_\beta}^6 - {m_e}^6)}. \tag{13}$$

In the expression, $Q_\beta = BE(Z+1, A) - BE(Z, A)$ is the β decay Q value for the sample (Z, A) which decays to the daughter $(Z+1, A)$ and $W_\beta = Q_\beta + {m_e}^2$. Here, $\rho_{\text{d.s.}}$ is the average density of states in the daughter nucleus ($e^{A/290}\times$ number of states within 1 MeV of ground state). The approach has been applied in Th an U isotopes[52] recently. It is important to note that all the daughter nuclei $(Z+1, A)$ involved in our calculation are odd-Z nuclei. In these cases, the time reversal

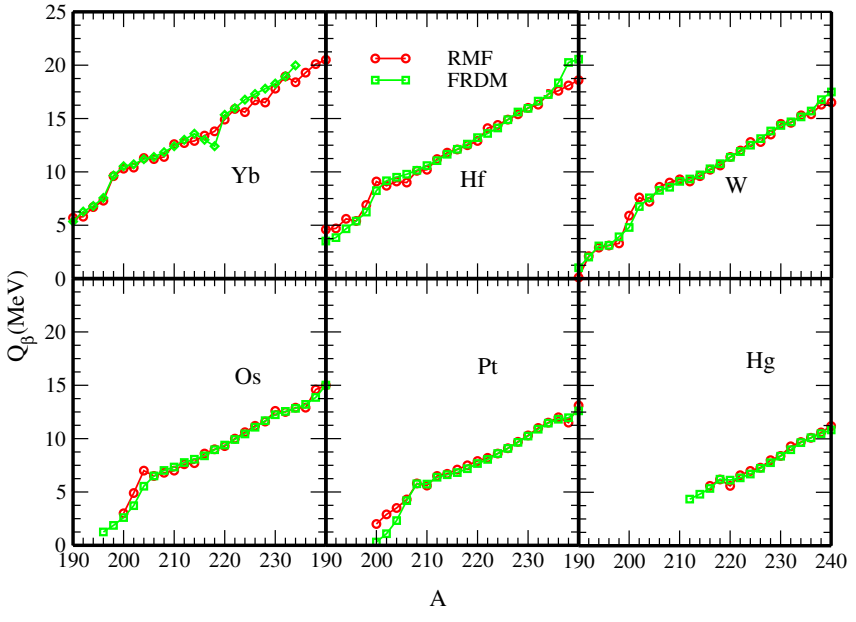

Fig. 9. The Q_β energy obtained from RMF(NL3)(circle) are compared with the FRDM(square) data for different isotopes in $Z = 70-80$ region.

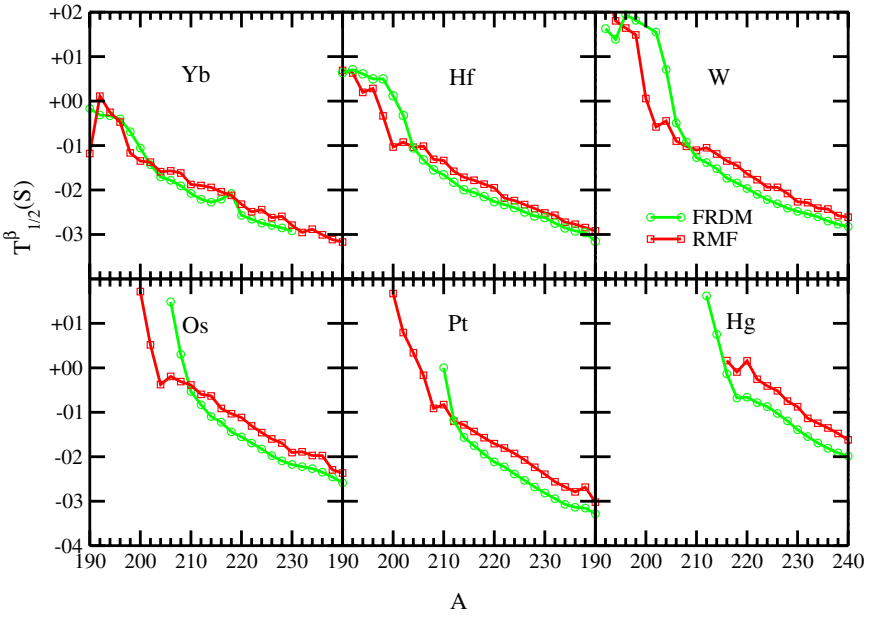

Fig. 10. The $T^\beta_{1/2}$ obtained from RMF(NL3)(circle) are compared with FRDM(square) data in $Z = 70-80$ region.

symmetry gets violated in the mean field models.[46,52] Therefore, to evaluate the BE of odd-Z nuclei, we used the Pauli blocking prescription[46] which restores the time-reversal symmetry. In Figs. 9 and 10, our results for Q_β and $T^\beta_{1/2}$ are displayed, respectively. For comparison, FRDM results are also given. One can see that RMF results almost follow the similar trend as that of FRDM results which confirms the applicability of the above formula[60] in $Z = 70-80$ mass region. Further, from Fig. 10, we can conclude that the decay of these nuclei mainly choose β decay as the prominent path.

5. Summary and Conclusion

We have calculated quadrupole deformation, hexadecoupole deformation, two-neutron separation energy and differential variation of two-neutron separation energy for some neutron-rich even–even nuclei in $Z = 70-80$ region using RMF theory with pairing correlation from BCS approach (RMF-BCS). The results from S_{2n} and dS_{2n} confirm the neutron shell closure at $N = 82$ and 126. As a further confirmatory test, the single particle energy levels for neutrons in isotopic chains are examined. We observed large gaps at $N = 82$ and 126. We have also calculated half-lives for α and β decay and seen that neutron-rich nuclei prefer β decay rather than going to α decay mode. Further, we concluded that the RMF-BCS theory provides a reasonably good description for all the considered isotopes.

Acknowledgment

The author S. Mahapatro thanks Institute of Physics, Bhubaneswar, India for providing library and computer facilities for these calculations.

References

1. I. Hamamoto, *Phys. Rev. C* **85** (2012) 064329.
2. T. Boumann, A. Spyrou and M. Theonnessen, *Rep. Prog. Phys.* **75** (2012) 036301.
3. P. J. Nolan and P. J. Twin, *Annu. Rev. Nucl. Part. Sci.* **38** (1988) 533.
4. S. Åberg, H. Flocard and W. Nazarewicz, *Annu. Rev. Nucl. Part. Sci.* **40** (1990) 439.
5. C. Baktash, B. Haas and W. Nazarewicz, *Annu. Rev. Nucl. Part. Sci.* **45** (1995) 485.
6. C. Baktash, *Prog. Part. Nucl. Phys.* **38** (1997) 291.
7. P. J. Twin, B. M. Nyakó, A. H. Nelson, J. Simpson, M. A. Bentley, H. W. Cranmer-Gordon, P. D. Forsyth, D. Howe, A. R. Mokhtar, J. D. Morrison, J. F. Sharpey-Schafer and G. Slethen, *Phys. Rev. Lett.* **57** (1986) 811.
8. P. Quentin and H. Flocard, *Annu. Rev. Nucl. Part. Sci.* **28** (1978) 23.
9. M. Baranger and K. Kumar, *Nucl. Phys. A* **110** (1968) 410.
10. G. D. Alkhazov *et al.*, *Nucl. Phys. A* **504** (1989) 549.
11. C. Thibault *et al.*, *Nucl. Phys. A* **367** (1981) 1.
12. I. Y. Lee *et al.*, *Phys. Rev. Lett.* **39** (1974) 682.
13. S. K. Patra and P. K. Panda, *Phys. Rev. C* **47** (1993) 1514.
14. M. M. Sharma and P. Ring, *Phys. Rev. C* **46** (1992) 1715.
15. B. Kumar, S. K. Singh and S. K. Patra, *Int. J. Mod. Phys. E* **24** (2015) 1550017.

16. E. Bashandy and M. S. El-Nesr, *Z. Naturforsch. A* **29** (2014) 1125.
17. P. R. John *et al.*, *Phys. Rev. C* **90** (2014) 021301(R).
18. G. A. Lalazissis, S. Raman and P. Ring, *At. Data Nucl. Data Tables* **71** (1999) 1.
19. P. Dabkiewicz *et al.*, *Phys. Lett. B* **82** (1979) 199.
20. M. Girod and J. P. Delaroche, *Phys. Rev. C* **45** (1993) 1420.
21. Y. K. Gambhir, P. Ring and A. Thimet, *Ann. Phys.* (*NY*) **198** (1990) 132.
22. S. K. Patra and C. R. Praharaj, *Phys. Rev. C* **44** (1991) 2552.
23. J. D. Walecka, *Ann. Phys.* (*NY*) **83** (1974) 491.
24. B. D. Serot and J. D. Walecka, *Adv. Nucl. Phys.* **16** (1986) 1.
25. C. J. Horowitz and B. D. Serot, *Nucl. Phys. A* **368** (1981) 503.
26. J. Boguta and A. R. Bodmer, *Nucl. Phys. A* **292** (1977) 413.
27. C. E. Price and G. E. Walker, *Phys. Rev. C* **36** (1987) 354.
28. T. Niksic *et al.*, *Prog. Part. Nucl. Phys.* **66** (2011) 519.
29. G. A. Lalazissis, J. König and P. Ring, *Phys. Rev. C* **55** (1997) 1.
30. S. K. Patra, *Phys. Rev. C* **48** (1993) 1449.
31. M. A. Preston and R. K. Bhaduri, *Structure of Nucleus* chap. 8 (Addison-Wesley Publishing Company, US, 1982) P. 309.
32. D. G. Madland and J. R. Nix, *Nucl. Phys. A* **476** (1981) 1.
33. P. Möller and J. R. Nix, *At. Data Nucl. Data Tables* **39** (1988) 213.
34. G. A. Lalazissis, M. M. Sharma and P. Ring, *Nucl. Phys. A* **597** (1996) 35.
35. K. Pomorski *et al.*, *Nucl. Phys. A* **624** (1997) 349.
36. P. Ring, *Prog. Part. Nucl. Phys.* **37** (1996) 193.
37. J. Dobaczewski, H. Flocard and J. Treiner, *Nucl. Phys. A* **422** (1984) 103.
38. J. Dobaczewski, W. Nazarewicz, T. R. Werner, J. F. Berger, C. R. Chinn and J. Decharge, *Phys. Rev. C* **53** (1996) 2809.
39. J. Meng *et al.*, *Prog. Part. Nucl. Phys.* **57** (2006) 470.
40. J. Meng, *Nucl. Phys. A* **635** (1998) 3.
41. M. Stoitsov, P. Ring, D. Vretenar and G. A. Lalazissis, *Phys. Rev. C* **58** (1998) 2086.
42. T. Nikšić, D. Vretenar, P. Ring and G. A. Lalazissis, *Phys. Rev. C* **65** (2002) 054320.
43. D. Vretenar, A. V. Afanasjev, G. A. Lalazissis and P. Ring, *Phys. Rep.* **409** (2005) 101.
44. P. Möller, J. R. Nix and K.-L. Kratz, *At. Nucl. Data Tables* **66** (1997) 131.
45. M. Wang, G. Audi, A. H. Wapstra, F. G. Kondev, M. Mac-Cormick, X. Xu and P. Pfeiffer, *Chin. Phys. C* **36** (2012) 1603.
46. S. K. Patra, M. Del Etal, M. Centelles and X. Vinas, *Phy. Rev. C* **63** (2001) 024311.
47. T. R. Werner, J. A. Sheikh, W. Nazarewicz, M. R. Strayer, A. S. Umar and M. Mish, *Phys. Lett. B* **335** (1994) 259.
48. T. R. Werner, J. A. Sheikh, M. Mish, W. Nazarewicz, J. Rikovska, K. Heeger, A. S. Umar and M. R. Strayer, *Nucl. Phys. A* **597** (1996) 327.
49. G. A. Lalazissis, D. Vretener, P. Ring, M. Stoitsor and L. M. Robledo, *Phys. Rev. C* **60** (1999) 014310.
50. G. A. Lalazissis, D. Vretenar, and P. Ring, *Nucl. Phys. A* **650** (1999) 133.
51. P. Arumugam, B. K. Sharma, S. K. Patra and Raj Kumar Gupta, *Phys. Rev. C* **71** (2005) 064308.
52. B. Kumar, S. K. Singh, S. K. Biswal, S. K. Patra, *Phys. Rev. C* **92** (2015) 054314.
53. Y. K. Gambhir, *Nucl. Phys. A* **570** (1994) 101.
54. P. Möller, J. R. Nix, W. D. Myers and W. J. Swiatecki, *At. Nucl. Data Tables* **59** (1995) 185.
55. S. Raman, C. W. Jr. Nestor and P. Tikkanen, *At. Nucl. Data Tables* **78** (2001) 1.
56. I. Angeli and K. P. Marinova, *At. Nucl. Data Tables* **99** (2013) 69.

57. S. K. Patra and C. R. Praharaj, *J. Phys. G* **23** (1997) 939.
58. V. E. Viola, Jr. and G. T. Seaborg, *J. Inorg. Nucl. Chem.* **28** (1966) 741.
59. A. Sobiczewski, Z. Patyk and S. C. Cwiok, *Phys. Lett B* **224** (1989) 1.
60. E. O. Fiset and J. R. Nix, *Nucl. Phys. A* **193** (1972) 647.